

Accepted for publication in the Astrophysical Journal Letters

# Using Chemistry to Unveil the Kinematics of Starless Cores: Complex Radial Motions in Barnard 68

Sébastien Maret, Edwin A. Bergin

*Department of Astronomy, University of Michigan, 500 Church Street, Ann Arbor, MI  
48109-1042, USA*

and

Charles J. Lada

*Harvard-Smithsonian Center for Astrophysics, 60 Garden Street, Cambridge, MA 02138,  
USA*

## ABSTRACT

We present observations of  $^{13}\text{CO}$ ,  $\text{C}^{18}\text{O}$ ,  $\text{HCO}^+$ ,  $\text{H}^{13}\text{CO}^+$ ,  $\text{DCO}^+$  and  $\text{N}_2\text{H}^+$  line emission towards the Barnard 68 starless core. The line profiles are interpreted using a chemical network coupled with a radiative transfer code in order to reconstruct the radial velocity profile of the core. Our observations and modeling indicate the presence of complex radial motions, with the inward motions in the outer layers of the core but outward motions in the inner part, suggesting radial oscillations. The presence of such oscillation would imply that B68 is relatively old, typically one order of magnitude older than the age inferred from its chemical evolution and statistical core lifetimes. Our study demonstrates that chemistry can be used as a tool to constrain the radial velocity profiles of starless cores.

*Subject headings:* astrochemistry – stars: formation — ISM: abundances — ISM: molecules — ISM: individual (Barnard 68)

## 1. Introduction

Starless cores likely represent the earliest stage of the formation of a star. In the standard view of star formation, cores form out an initially magnetically sub-critical cloud, and evolve

in a quasi-static fashion through ambipolar diffusion (Shu et al. 1987; Mouschovias & Morton 1991). In the opposite picture, cores are dynamic objects that form by shocks in a turbulent flow, fragment and collapse (or disappear) in a few crossing times (Padoan et al. 2001; Ballesteros-Paredes et al. 2003). Velocity measurements can provide important constraints on these two scenarios. For example, Tafalla et al. (1998) examined the kinematics of L1544 and inferred infall velocities up to  $0.1 \text{ km s}^{-1}$  *a priori* incompatible with sub-critical ambipolar diffusion models. However, Ciolek & Basu (2000) argued that these velocities can be understood if the core is super-critical.

Line of sight velocities in cores can be established from observations of self-absorbed line profiles. In an infalling core, if the excitation temperature increases towards the center (as one can expect in a centrally condensed core with a roughly constant temperature), self-absorbed lines are expected to be asymmetric, with a blue peak brighter than the red peak (see Evans 1999). This technique has been used in the past to detect collapse motions in starless cores and protostars (see Myers et al. 2000, for a review). One of the major difficulties of this technique is the large degree of chemical complexity within these objects. For example, numerous molecules are observed to deplete in the densest regions of starless cores (e.g. Bergin et al. 2002; Tafalla et al. 2002), thus hampering our ability to measure the velocity in the dense central regions of these objects.

Nevertheless, with a detailed knowledge of the chemistry of these objects, one can choose appropriate molecular transitions to trace different part of the cores, and unveil their radial kinematic structure (Bergin 2003; van der Tak et al. 2005). In this paper, we use line observations of  $^{13}\text{CO}$ ,  $\text{C}^{18}\text{O}$ ,  $\text{HCO}^+$ ,  $\text{H}^{13}\text{CO}^+$ ,  $\text{DCO}^+$  and  $\text{N}_2\text{H}^+$  to reconstruct the velocity profile of the Barnard 68 core (hereinafter B68). With a well defined physical (Alves et al. 2001; Bergin et al. 2006) and chemical (Bergin et al. 2002; Maret et al. 2006; Maret & Bergin 2007) structure, this core is an ideal target for such a study. For this we compare the observed line profiles with the predictions of a chemical network coupled with a radiative transfer code. The paper is organized as follow. Observations are presented in §2. The analysis is detailed in §3, and the results are discussed in §4.

## 2. Observations

Maps of  $\text{H}^{13}\text{CO}^+$  (1-0) ( $\nu = 86.754288 \text{ GHz}$ ),  $\text{HCO}^+$  (1-0) ( $\nu = 89.188523 \text{ GHz}$ ),  $\text{N}_2\text{H}^+$  (1-0) ( $\nu = 93.173772 \text{ GHz}$ )  $\text{C}^{18}\text{O}$  (1-0) ( $\nu = 109.782173 \text{ GHz}$ ),  $\text{DCO}^+$  (2-1) ( $\nu = 144.077289 \text{ GHz}$ ),  $\text{DCO}^+$  (3-2) ( $\nu = 216.112604 \text{ GHz}$ ) and  $\text{HCO}^+$  (3-2) ( $\nu = 267.557526 \text{ GHz}$ ) transitions were observed towards B68 ( $\alpha = 17^{\text{h}}22^{\text{m}}38.2^{\text{s}}$  and  $\delta = -23^{\circ}49'34.0''$ ; J2000) in April 2002 and September 2002 with the IRAM-30m telescope. The  $^{13}\text{CO}$  (2-1) ( $\nu =$

220.398684 GHz) transition was observed in September 2003 with the *Caltech Submillimeter Observatory* (CSO). These observations have already been presented in Bergin et al. (2002), Bergin et al. (2006), Maret et al. (2006), and Maret & Bergin (2007), and we refer the reader to these papers for technical details.

Transitions of  $\text{HCO}^+$  (4-3) ( $\nu = 356.734134$  GHz) and  $\text{N}_2\text{H}^+$  (3-2) ( $\nu = 279.511832$  GHz) were observed in August 2005 using the *Atacama Pathfinder eXperiment* telescope (APEX). The APEX-2A receiver was used together with the FFTS spectrometer, which provides a spectral resolution of 61 kHz. The telescope half power beam size is  $22''$  at 280 GHz and  $17''$  at 357 GHz. The data were calibrated using the chopper wheel method, and the system temperature was  $\sim 100$  K at 280 GHz and 130-180 K at 357 GHz. The observations were converted on the  $T_{\text{mb}}$  scale assuming a main beam efficiency of 70% and a forward efficiency of 95% (C. de Breuck, priv. comm.). These observations were obtained in beam switching mode.

Fig. 1 present the observations together with our model predictions (see § 3 for a description of the model). The lines show a variety of different profiles, from Gaussian to self-absorbed and asymmetric double peaked profiles.  $\text{C}^{18}\text{O}$ ,  $^{13}\text{CO}$  and  $\text{H}^{13}\text{CO}^+$  are probably optically thin (or only moderately optically thick), and have centrally peaked Gaussian profiles. On the other hand,  $\text{HCO}^+$  (1-0) and (3-2) lines are self-reversed and show the typical blue asymmetry (blue peak brighter than the red peak). These line profiles suggests that collapsing motions are present along the line of sight. Surprisingly, self-absorbed  $\text{HCO}^+$  (4-3),  $\text{DCO}^+$  (3-2), and the central component of the  $\text{N}_2\text{H}^+$  (1-0) line exhibit red asymmetry (red peak brighter than the blue peak), indicating expansion. Finally, the  $\text{DCO}^+$  (2-1) line is self-absorbed but symmetric, hinting at the presence of static gas along the line of sight. The absorption dip velocity of self-reversed lines is consistent with the  $v_{\text{LSR}}$  of the source ( $3.31 \text{ km s}^{-1}$ ), as determined from the  $\text{C}^{18}\text{O}$  (1-0) line. In the following, we model the line profiles in order to constrain the line-of-sight velocity of the core.

### 3. Analysis and results

We have modelled the spectral line profiles shown on Fig. 1 following the approach described in Bergin et al. (2006), Maret et al. (2006) and Maret & Bergin (2007). The abundance profiles were computed using a chemical network that includes gas grain interactions, as well as the fractionation reactions for carbon, oxygen, and deuterium (Bergin & Langer 1997). These abundance profiles were used to compute the line emission using a 1-D Monte Carlo radiative transfer code (Ashby et al. 2000). These model predictions were convolved at the appropriate spatial resolution in order to be compared with the observations, assuming

a distance of 125 pc.

The density profile from Alves et al. (2001) and the gas and dust temperature from Bergin et al. (2006) were used. We have adopted the same initial abundances and cosmic ionization rate as in the Maret & Bergin (2007) “best-fit” model. As a first approach, we have assumed that no systematic radial motions are present in the core. We have used the turbulent velocity profile determined by Bergin et al. (2006) from C<sup>18</sup>O (1-0) line observations. The turbulent velocity contribution is 0.3 km s<sup>-1</sup> (FWHM) at the surface of the core, and decreases towards the center down to 0.15 km s<sup>-1</sup>. Rotation of the cloud has been neglected. Both the <sup>13</sup>CO (2-1) and the H<sup>13</sup>CO<sup>+</sup> (1-0) lines have an unresolved hyperfine structure that need to be taken into account in order to properly model the line profiles. Following the approach used by Tafalla et al. (2006), we have artificially broadened these two lines by 0.13 km s<sup>-1</sup>, which corresponds to the separation between the two hyperfine components of each species (Schmid-Burgk et al. 2004).

On Fig. 2, we present the abundances predicted by our chemical model. From this figure we can roughly estimate which lines originate in different parts of the core. For example, the HCO<sup>+</sup> abundance peaks in the outer part of the core ( $A_v \sim 2$ ) and decreases towards the center because of the freeze-out of its parent molecule CO. Consequently, HCO<sup>+</sup> lines probe predominantly the outer layer. Both N<sub>2</sub>H<sup>+</sup> and DCO<sup>+</sup> abundances peak deeper inside, at an  $A_v$  of 5 and 13 respectively. Therefore lines from these two species preferentially trace the inner regions of the core. Of course, excitation effects are also important, and different transitions of the same molecule are expected to probe different depths in the core as well. For example, the HCO<sup>+</sup> (4-3) opacity is likely lower than the (1-0) and (3-2) lines, and thus the HCO<sup>+</sup> (4-3) line probably arises from deeper regions than the HCO<sup>+</sup> (3-2) and (1-0) lines. Altogether, our observations suggest the presence of complex radial motions in B68, with inwards motions in the outer part of the core – as indicated by the blue HCO<sup>+</sup> (1-0) and (3-2) line profiles – and outward motions in the inner region – as shown by the HCO<sup>+</sup> (4-3), DCO<sup>+</sup> (3-2) and N<sub>2</sub>H<sup>+</sup> (1-0) lines. In addition, the DCO<sup>+</sup> (2-1) line hints at the presence of an intermediate static region between these two parts.

In order to test this hypothesis, we have computed the line profiles for the step-like velocity profile represented on Fig. 3. By convention, negative velocities correspond to inward motions, while positive velocities correspond to outward motions. The velocity is assumed to be negative (-0.045 km s<sup>-1</sup>) at radius greater than 8,000 AU, and positive (0.025 km s<sup>-1</sup>) at smaller radii. Fig. 1 compares the observations with our model predictions for this velocity profile. The fit is not perfect. However, given the complexity of our modeling – chemical network coupled with a radiative transfer model – the overall agreement between the model predictions and observations is fairly good. The model reproduces quite well the

infall asymmetry of  $\text{HCO}^+$  (1-0) and (3-2), as well as the blue asymmetry of the (4-3) line.  $\text{H}^{13}\text{CO}^+$  (1-0),  $\text{N}_2\text{H}^+$  (3-2),  $\text{C}^{18}\text{O}$  (1-0) and  $^{13}\text{CO}$  (2-1) line profiles are also well matched. Although the model predicts correct integrated intensities for  $\text{DCO}^+$  (3-2) and  $\text{N}_2\text{H}^+$  (1-0), it does not reproduce the blue asymmetries seen in these lines. The predicted line profiles have a Gaussian shape, whereas the observed lines are self-absorbed. In these cases, it appears that our model underestimates the opacity of these lines.

#### 4. Discussion and conclusions

Our observations and modelling indicate that the outer part of the core is collapsing while the inner part is expanding. The velocities in both regions are relatively small (a few tens of meters per second) and are largely sub-sonic. The transition between the collapsing and expanding region occurs at a radius of about 8,000 AU. It is important to note that the fit to the observations is probably not unique. However, large changes in the transition and velocities between the regions are likely ruled out. As already mentioned, our model does not reproduce the asymmetries of the  $\text{N}_2\text{H}^+$  (1-0) and  $\text{DCO}^+$  line profiles, due to an underestimating of the opacity. There are several possible explanations for this discrepancy. First, our chemical model might not predict the correct abundance profile for these two species. For example, increasing the  $\text{DCO}^+$  abundance at intermediate radii, with a subsequent reduction at small radii to keep the column density constant would increase the opacity of line without changing the line flux significantly (which is correctly predicted). Indeed, our model predicts a  $\text{DCO}^+$  (2-1) line intensity at  $10 < A_v < 20$  that is lower than observed (see Fig. 3 in Maret & Bergin 2007). Second, the physical structure of the core is also somewhat uncertain. For example, the temperature profile may be slightly different than the one predicted by Bergin et al. (2006) (see Crapsi et al. 2007), although small changes ( $\pm 3$  K) in the temperature profile were found to have little effect on the line intensities. Turbulence at the center of the core might also be different than what assumed here. The turbulent profile was determined by Bergin et al. (2006) using  $\text{C}^{18}\text{O}$  observations, which are not a good probe of the innermost regions of the core because of heavy depletion. Decreasing the turbulent velocity profile in the innermost region of the core would also increase the opacity of these two lines. Regardless of the discrepancy with our model predictions, we emphasize these two line profiles, together with the  $\text{HCO}^+$  (4-3) line profile, unambiguously indicate the presence of outwards motions at the center of the core. We found that no constant infalling velocity profile could reproduce the observations.

The step-like velocity profile we obtain is suggestive of the presence of radial oscillations in the core. Small non-radial oscillations of the outer layers of the core around a stable equi-

librium have been proposed by Lada et al. (2003) and Redman et al. (2006) to interpret the asymmetry of the CS (2-1) and HCO<sup>+</sup> (3-2) lines observed in Barnard 68. Lada et al. (2003) also suggested that, in addition to the surface oscillations seen in the CS (2-1) line, some radial oscillation might also be present. Our observations and modeling are in agreement with this hypothesis.

Keto & Field (2005) proposed a hydrodynamic model for the evolution of cores in quasi-equilibrium. In their modeling, a small perturbation of a stable core (according to the Bonnor-Ebert criterion) is found to result in damped oscillations around the equilibrium position. Keto et al. (2006) showed that the surface pattern observed in the CS (2-1) line towards B68 is consistent with the ( $n = 1, l = m = 2$ ) quadripolar oscillation mode for a specific orientation ( $\lambda = \theta = 30^\circ$ ). For the same oscillation mode, the radial velocity is qualitatively similar to the one obtained in this study, but is out of phase: the inner part of the core has a negative radial velocity, while the outer part of the core has a positive velocity. At the other half of the oscillation cycle, the velocity would be reversed and in qualitative agreement with the profile we obtain (E. Keto, *priv. comm.*)

As pointed out by Keto et al. (2006) and Redman et al. (2006), the presence of oscillations in B68 suggests that the core is relatively old, typically older than a few sound speed crossing times ( $\sim 10^6$  yr). This is comparable to the ambipolar diffusion timescale at the center of the core and more than one order of magnitude higher than the free-fall time scale ( $10^6$  and  $7 \times 10^4$  yr respectively; Maret & Bergin 2007). This is also about an order of magnitude higher than the age of the core as determined from the degree of CO depletion ( $10^5$ yr; Bergin et al. 2002, 2006)<sup>1</sup>. For  $t = 3 \times 10^5$  yr, Bergin et al. (2006) model predicts a C<sup>18</sup>O (1-0) line intensity that is three times smaller than the observations, while at  $t = 10^6$  yr, the greater CO depletion leads to an even greater mismatch between observations and model predictions. The N<sub>2</sub>H<sup>+</sup>, HCO<sup>+</sup>, H<sup>13</sup>CO<sup>+</sup>, and DCO<sup>+</sup> would also be underestimated by the model because of the freeze-out of their parent or their precursors, N<sub>2</sub>, CO and <sup>13</sup>CO. Thus the “chemical age” of B68 inferred from the CO depletion appears to be hard to reconcile with the “dynamical age” implied by the presence of surface oscillations. It is also interesting to compare the sound crossing time in B68 to typical statistical starless core lifetimes (see Ward-Thompson et al. 2007, for a review). Using sub-millimeter continuum emission maps, Kirk et al. (2005) obtained lifetimes of  $1 - 3 \times 10^5$  years which are in good agreement with the age of the B68 determined from CO depletion, but again about an order of magnitude higher than the sound crossing time.

---

<sup>1</sup>Strictly speaking, the age determined by this method is a lower limit of the real age of the cloud, because CO is assumed to be pre-existing, and the density is supposed to be constant (Bergin et al. 2006).

The present study emphasizes the importance of understanding the chemistry to constrain the kinematics of starless using spectral line profiles. Because of the strong chemical gradients that exist in these cores – as well as excitation effects – different lines can be used to selectively trace different parts of the core. We have demonstrated that, using lines that are appropriately chosen, it is possible to reconstruct the core radial velocity profile. In B68, our observations and modelling suggest the presence of complex line-of-sight motions that are consistent radial oscillations. The presence of such oscillation indicates that some core are long-lived, with lifetimes about an order of magnitude higher than those derived from their chemical evolution or sub-millimeter surveys. So far, oscillations have been inferred in only one other core, FeSt 1-457 (Aguti et al. 2007). Clearly, similar studies on a larger number of cores are needed to establish if such cores are common.

S. M. wishes to thank Eric Keto for fruitful discussions. The authors are also grateful to the referee for useful and constructive comments. This work is supported by the National Science Foundation under grant 0335207.

*Facilities:* IRAM:30m, CSO, APEX

## REFERENCES

- Aguti, E. D., Lada, C. J., Bergin, E. A., Alves, J. F., & Birkinshaw, M. 2007, ApJ, in press
- Alves, J. F., Lada, C. J., & Lada, E. A. 2001, Nature, 409, 159
- Ashby, M. L. N., Bergin, E. A., Plume, R., Carpenter, J. M., Neufeld, D. A., Chin, G., Erickson, N. R., Goldsmith, P. F., Harwit, M., Howe, J. E., Kleiner, S. C., Koch, D. G., Patten, B. M., Schieder, R., Snell, R. L., Stauffer, J. R., Tolls, V., Wang, Z., Winnewisser, G., Zhang, Y. F., & Melnick, G. J. 2000, ApJ, 539, L115
- Ballesteros-Paredes, J., Klessen, R. S., & Vázquez-Semadeni, E. 2003, ApJ, 592, 188
- Bergin, E. A. 2003, in SFChem 2002: Chemistry as a Diagnostic of Star Formation, proceedings of a conference held August 21-23, 2002 at University of Waterloo, Waterloo, Ontario, Canada N2L 3G1. Edited by Charles L. Curry and Michel Fich. NRC Press, Ottawa, Canada, 2003, p. 63., ed. C. L. Curry & M. Fich, 63–+
- Bergin, E. A., Alves, J. ., Huard, T., & Lada, C. J. 2002, ApJ, 570, L101
- Bergin, E. A. & Langer, W. D. 1997, ApJ, 486, 316

- Bergin, E. A., Maret, S., van der Tak, F. F. S., Alves, J., Carmody, S. M., & Lada, C. J. 2006, *ApJ*, 645, 369
- Bringa, E. M. & Johnson, R. E. 2004, *ApJ*, 603, 159
- Ciolek, G. E. & Basu, S. 2000, *ApJ*, 529, 925
- Crapsi, A., Caselli, P., Walmsley, M. C., & Tafalla, M. 2007, *A&A*, 470, 221
- Evans, N. J. 1999, *ARA&A*, 37, 311
- Hasegawa, T. I. & Herbst, E. 1993, *MNRAS*, 261, 83
- Keto, E., Broderick, A. E., Lada, C. J., & Narayan, R. 2006, *ApJ*, 652, 1366
- Keto, E. & Field, G. 2005, *ApJ*, 635, 1151
- Kirk, J. M., Ward-Thompson, D., & André, P. 2005, *MNRAS*, 360, 1506
- Lada, C. J., Bergin, E. A., Alves, J. F., & Huard, T. L. 2003, *ApJ*, 586, 286
- Maret, S. & Bergin, E. A. 2007, *ApJ*, 664, 956
- Maret, S., Bergin, E. A., & Lada, C. J. 2006, *Nature*, 442, 425
- Mouschovias, T. C. & Morton, S. A. 1991, *ApJ*, 371, 296
- Myers, P. C., Evans, N. J., & Ohashi, N. 2000, *Protostars and Planets IV*, 217
- Padoan, P., Juvela, M., Goodman, A. A., & Nordlund, Å. 2001, *ApJ*, 553, 227
- Redman, M. P., Keto, E., & Rawlings, J. M. C. 2006, *MNRAS*, 370, L1
- Roberts, J. F., Rawlings, J. M. C., Viti, S., & Williams, D. A. 2007, *ArXiv e-prints*, 708
- Schmid-Burgk, J., Muders, D., Müller, H. S. P., & Brupbacher-Gatehouse, B. 2004, *A&A*, 419, 949
- Shu, F. H., Adams, F. C., & Lizano, S. 1987, *ARA&A*, 25, 23
- Tafalla, M., Mardones, D., Myers, P. C., Caselli, P., Bachiller, R., & Benson, P. J. 1998, *ApJ*, 504, 900
- Tafalla, M., Myers, P. C., Caselli, P., Walmsley, C. M., & Comito, C. 2002, *ApJ*, 569, 815



Tafalla, M., Santiago-García, J., Myers, P. C., Caselli, P., Walmsley, C. M., & Crapsi, A. 2006, *A&A*, 455, 577

van der Tak, F. F. S., Caselli, P., & Ceccarelli, C. 2005, *A&A*, 439, 195

Ward-Thompson, D., André, P., Crutcher, R., Johnstone, D., Onishi, T., & Wilson, C. 2007, in *Protostars and Planets V*, ed. B. Reipurth, D. Jewitt, & K. Keil, 33–46

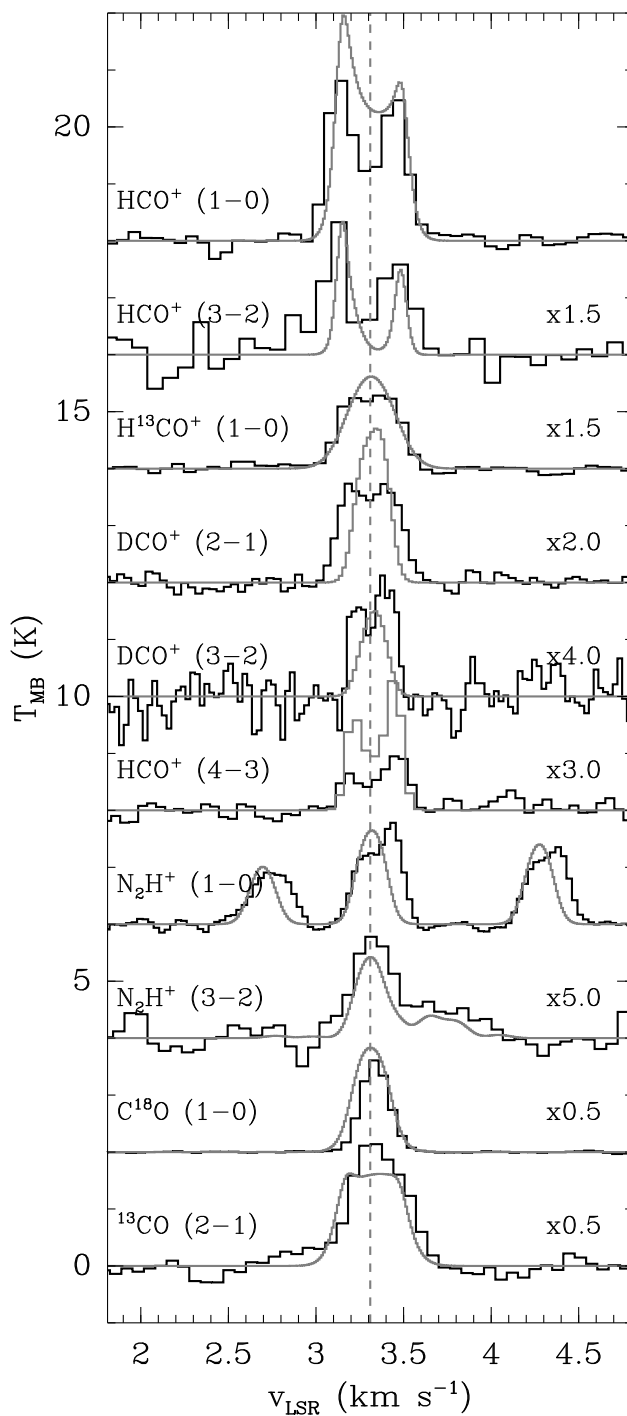


Fig. 1.— Comparison between the line profiles observed towards the extinction peak of B68 (black histograms) and the predictions of our “best fit” model (solid grey lines). For the clarity of the plot, lines are shifted vertically, and some of them are scaled by the factor mentioned on the right of each curve.

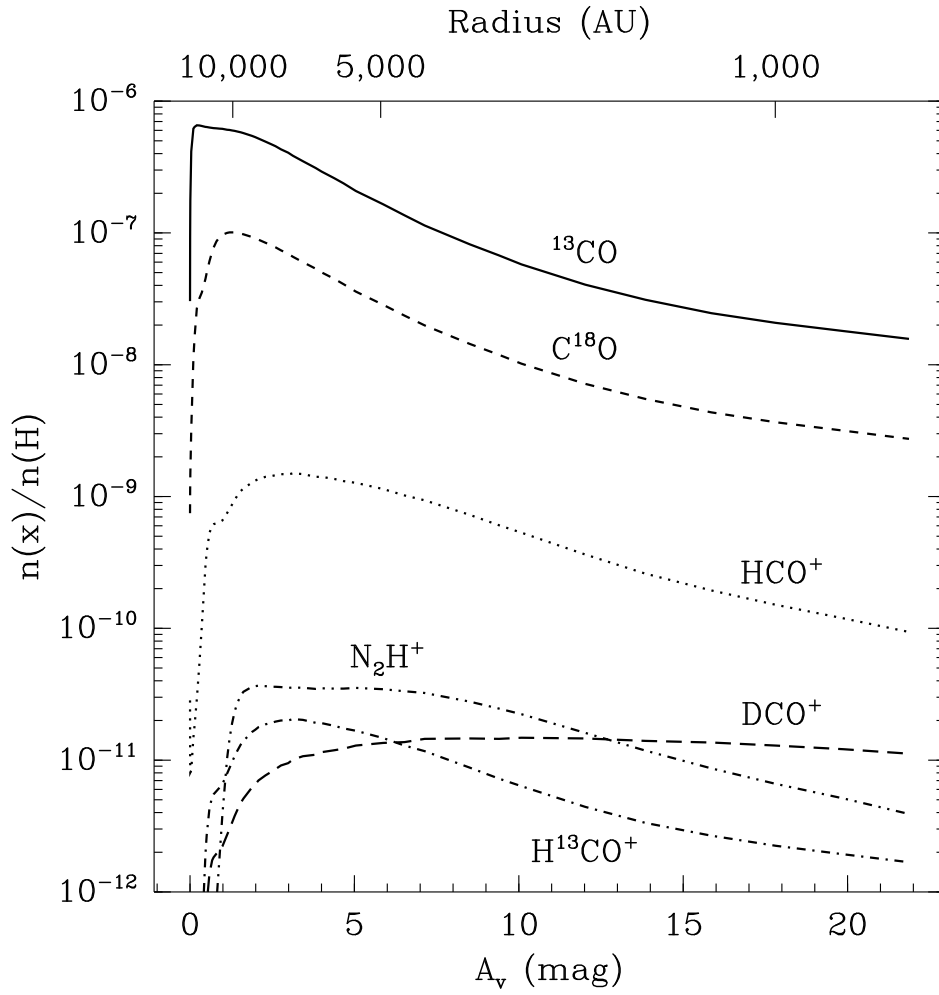


Fig. 2.— Abundances predicted by our chemical model for the observed species as a function of the visual extinction in the core.

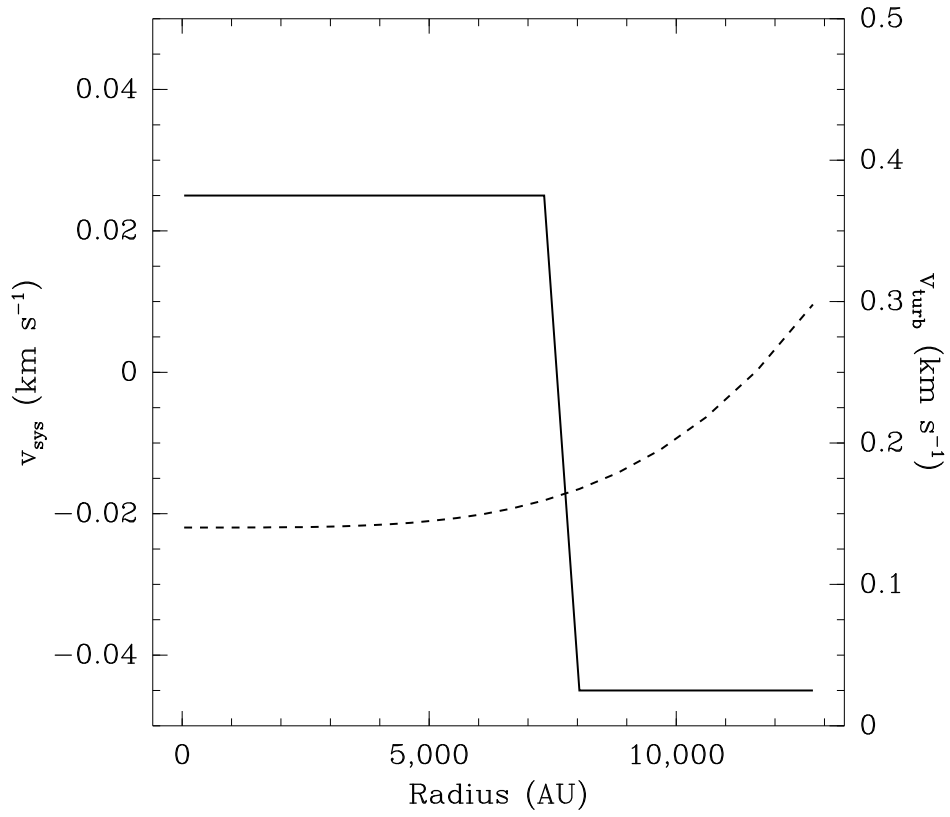


Fig. 3.— Best fit radial velocity profile. The solid line shows the systemic velocity profile (values are on the left axis). The dashed line shows the turbulent velocity profile (values are on the right axis, from Bergin et al. 2006).